Ultramicroscopy 186 (2018) 62–65

Contents lists available at ScienceDirect

Ultramicroscopy

journal homepage: www.elsevier.com/locate/ultramic

Fine tuning an aberration corrected ADF-STEM

Earl J. Kirkland

School of Applied and Engineering Physics Cornell University Ithaca, NY 14853 USA

ARTICLE INFO

Article history:
Received 7 January 2017
Accepted 1 December 2017
Available online 12 December 2017

Keywords:
STEM
ADF-STEM
Aberration corrector
Autofocus
Tuning

ABSTRACT

Aberration correctors offer greatly enhanced resolution in electron microscopes, however can require dramatically more complicated adjustments. A method of computer adjustment of a probe forming aberration corrector in a Scanning Transmission Electron Microscope (STEM) is proposed and analyzed using image simulation. This method works directly with the image and should work well with crystalline specimens. It does not have a significant dependence on post specimen lens aberrations.

1. Introduction

Multipole aberration correctors have significantly enhanced the resolution of modern transmission electron microscopes (TEM). Hawkes [1] and Rose [2] have reviewed the recent history of aberration corrector developments. To correct a few aberrations, multipole correctors add many other parasitic multipole aberrations that also must be correcting, leaving dozens of extra aberration controls to be adjusted. There are too many controls to be practical to adjust manually in a reasonable amount of time, so typically require computer automation of the focusing or tuning process to adjust all of the controls.

The process of adjusting the corrector may be referred to as tuning or focusing. High order aberration may not change significantly in many days and the lower orders may require frequent adjustment on a time scale of an hour or so.

CTEM (Conventional or parallel beam TEM) aberrations may be analyzed and adjusted using a series of images recorded at different beam tilts similar to a Zemlin tableau (Uhlemann and Haider [3], Sawada [4]). This may require adjustment using a separate specimen in some cases.

Many methods of STEM (Scanning TEM) tuning analyze the Ronchigram or projection image formed by a fixed convergent probe at large defocus. Krivanek et al. [5] and Dellby et al. [6] describe a method of analyzing the shift of small patches in the Ronchigram to analyze the local magnification and hence the aberrations. Sawada et al. [7,8] have described a tuning method analyzing the autocorrelation function of different regions of the Ronchigram and images. Any Ronchigram based method will have the disadvantage of being very dependent on the aberrations of the post specimen lens which must be accurately characterized. Some methods of tuning using Ronchigrams of amorphous and crystalline specimens have been reviews by Lupini et al. [9–11].

2. Aberrations

Aberrations may be characterized by the phase error across the objective aperture. There are several different functions that can be used. Most currently favored methods have a similar form but different notation. The aberration function using the notation of Krivanek et al. [5,12] that will be used here is:

$$\chi(\alpha,\phi) = \frac{2\pi}{\lambda}\sum_{mn}\frac{\alpha^{n+1}}{n+1}[C_{nma}\cos(m\phi) + C_{nmb}\sin(m\phi)] \quad (1)$$

where n and m are positive integers and zero and $m \le n+1$. α is the polar angle and ϕ is the azimuthal angle. λ is the wavelength of the electron. For example C_{30} is spherical aberration (C_3) and C_{23} is three fold astigmatism (A_2). This notation is compared to other possible symbol choices by Erni[13], and Kirkland [14,15].

The traditional maximum allowed error is $\pi/4$ in each aberration at the maximum angle (outer circumference of the objective aperture). For simplicity ignore the azimuthal dependence (or equivalently look only in the maximum direction) and equate the residual aberration (i.e. maximum allowed error) as:

$$\left|\frac{2\pi}{\lambda}\frac{\alpha_{max}^{n+1}}{n+1}C_{nm}\right| \le \frac{\pi}{4} \quad (2)$$

$$\left|C_{nm}\right| \le T_n = \frac{(n+1)}{8\alpha_{max}^{n+1}}\lambda \quad (3)$$

E-mail address: ejk14@cornell.edu

https://doi.org/10.1016/j.ultramic.2017.12.002
0304-3991/

Table 1
Maximum allowed tuning errors for 30 mrad. objective aperture (Eq. (3)) and 100keV ($\lambda = 0.03701$ Ang.).

Aberration	expression	100keV
C_{1m}	$2\lambda/(8\alpha^2)$	1.02 nm
C_{2m}	$3\lambda/(8\alpha^3)$	51.4 nm
C_{3m}	$4\lambda/(8\alpha^4)$	2.28 µm
C_{4m}	$5\lambda/(8\alpha^5)$	95.2 µm
C_{5m}	$6\lambda/(8\alpha^6)$	3.81 mm

where T_n is the tolerance or maximum allowed error in aberrations C_{nm} of order n. Some values are shown in Table 1.

3. Autofocus

Erasmus [16] and Saxton et al. [17] proposed using the image variance as a means of focusing and stigmating in the SEM and CTEM. This method was also verified for the ADF-STEM (ADF meaning annular dark field, in which only the electrons scattered to high angles are collected by the detector) by Kirkland [18]. ADF-STEM imaging of thin specimens has a fairly simple relationship to specimen structure similar to an incoherent image. Higher order aberration should reduce image contrast similarly to astigmatism and defocus, so it is reasonable to expect the image variance (or contrast) to be a maximum when the aberration are minimized. The variance will also include the noise in the image but the noise statistics should not change appreciably as the aberrations are varied.

The total image variance is just the square of the standard deviation of the values in the pixels of the image. Dividing the variance by the square of the mean value of the image will reduce the sensitivity to slow drift in beam current and specimen position. A figure of merit is defined as:

$$F(C_{nm}) = \frac{\sigma^2}{\mu^2} = \text{MAX} \tag{4}$$

where σ^2 is the image variance (square of the standard deviation σ) and μ is the mean value of the image.

$$\mu = \frac{1}{N}\sum_{ij} z_{ij} \tag{5}$$

$$\sigma^2 = \frac{1}{N}\sum_{ij}\left[z_{ij} - \mu\right]^2 = \frac{1}{N}\sum_{ij} z_{ij}^2 - \left[\frac{1}{N}\sum_{ij} z_{ij}\right]^2 \tag{6}$$

where z_{ij} is the value of the image pixel at position (i, j) and N is the total number of pixels in the image. The dependence of F on C_{nm} is an abbreviation for all of the relevant aberrations. Using the ADF-STEM image directly has the advantage of being relatively insensitive to any post specimen lens aberration (unless severe enough to significantly change the apparent detector geometry).

With the assumption that the microscope has been mostly aligned (lenses centered etc.) and tuned well enough to obtain an image, the normalized image variance might be used to fine tune the final configuration. The specimen is also assumed to be thin and remain mostly unchanged during tuning (without significant radiation damage or drift). The figure of merit, Eq. (4), can be treated as a N-dimensional optimization problem (where N=12 for third order tuning). The aberration corrector on the microscope is assumed to have a control for each of the aberrations that can be changed from a computer program which is also able to acquire images in the same program.

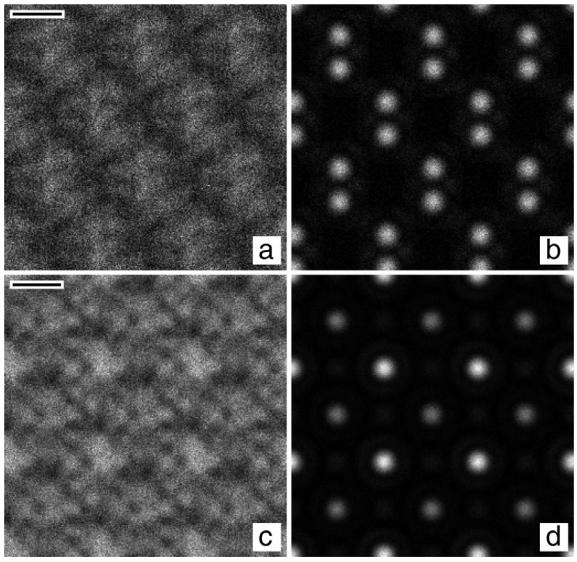

Fig. 1. Auto fine focus (100 kV, probe current 70 pAmp and dwell time 16µs, 30 mrad. objective aperture, 50Å defocus spread, detector angles 80 to 200 mrad). a,b) 3x2x3 unit cells of 110 Si. c,d) 3x3x3 unit cells of $SrTiO_3$. a,c) starting image with random aberration errors between $\pm 10T_n$ for 12 aberrations to third order, b,d) final tuned image. (scale bar 0.2 nm).

There are many well developed algorithms for optimization. However, there are only two [19,20] that do not directly require calculating derivatives which would be unsuitable for noisy data. Of these, the non-linear simplex method of Nedler and Mead [20] (not to be confused with the linear-programming method of the same name) seems to tolerate some level of noise and unsmooth functions as in typical ADF-STEM images. This is a minimization algorithm but can be used to find the maximum by using the negative of the figure of merit. The relative scale of defocus (C_{10}) and spherical aberration (C_{30}) are very different. Most optimization algorithms will work better if all independent parameters are on the same scale. It is advantageous to scale each aberration C_{nm} with its tolerance as in Table 1. The independent variable used in the optimization procedure are C_{nm}/T_n and the figure of merit becomes $F(C_{nm}/T_n)$.

The simplex method works by first taking a small step in each of the N independent directions or parameters and evaluating the figure of merit at these positions. This set of N directions and values is the so-called simplex. It then uses a clever method of estimating a new optimal direction to move to get a better result using the previous results. This process is repeated until the function no longer gets smaller. For tuning, this has the added advantage that the aberration controls would not need to be precisely calibrated. The N aberration controls just have to be independent and span the required space of aberrations. The trial step process will tend to discover what each aberration control really does, assuming that the specimen remains stable. Usually once the simplex method has converged it is recommended to try one restart from the current position to ensure convergence. One restart is used here.

An image of 3 x 2 x 3 unit cells of 110 Silicon is used as a test specimen is shown in Fig. 1. The image is calculated in the incoherent image model [15,21]. This is a thin specimen with low atomic number so is fairly well described in the incoherent image model which is dramatically easier to calculate. (It is not practical, or necessary, to calculate a full multislice simulation of a thick specimen with the available computers.) Noise may be significant and may interfere with many optimization procedures. The images include

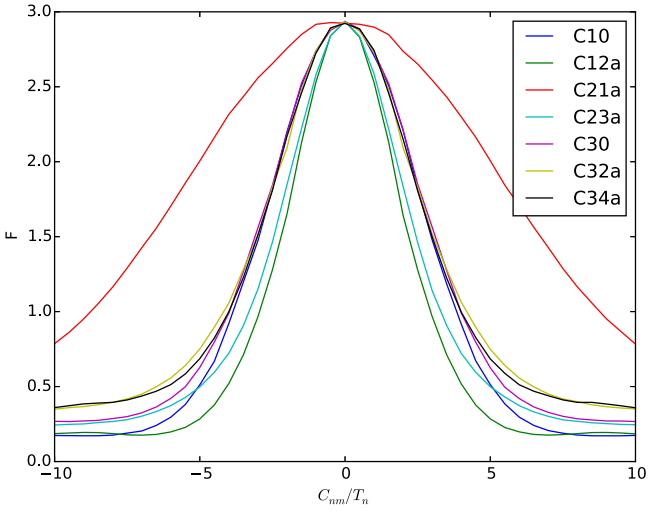

Fig. 2. Calculated dependence of the figure of merit versus scaled aberration values (100 kV, probe current 70 pAmp and dwell time 16μs) using the Si 110 test image.

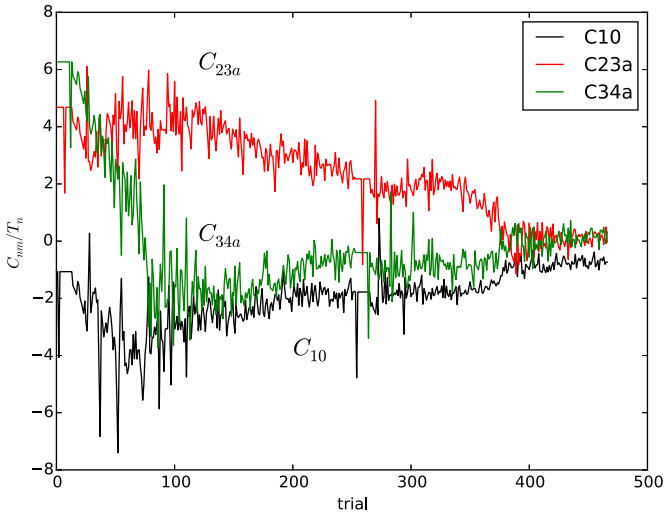

Fig. 3. Trial values of some aberrations as the simplex method progresses, for the 110 Si image with 12 aberrations (to third order). These include the search values surrounding the current optimum value.

Poisson electron counting noise (different for each successive image) for a typical beam current and dwell time and also a small defocus spread (chromatic aberration). To be practical as a tuning method, any test images must be small to be acquired quickly, so this calculation is performed with 256 by 256 pixel images. The simplex method was run until the standard deviation of the final simplex (last N+1 values tested) is approx. 0.01 of the average value. This is a fairly high value (less accurate) which is necessary with noise in the data. The starting image has random errors in the aberrations in the range $\pm 10T_n$ which may be a worst case example of this fine tuning procedure. The starting image Fig. 1a is not good, but maximizing the total variance (Eq. (4)) produces a focused image in Fig. 1b which is greatly improved, revealing the familiar dumbbell pairs of Si atoms. Fig. 1c,d are similar but for strontium titanate ($SrTiO_3$).

To be more precise the figure of merit is plotted versus the aberration coefficients scaled to the tolerance for each aberration (Eq. (3)) in Fig. 2. Each aberration was varied one at a time with all other aberrations held at zero using the same image as in Fig. 1a,b. For simplicity the C_{nmb} aberrations are omitted because they will be substantially similar to the C_{nma} aberrations. Coma (C_{21}) is not particularly sensitive because it can be compensated with shift (C_{01}) which is not important. It is interesting that all curves are similar when scaled to the tolerance. Each curve has a single well defined maximum which is very good for convergence and is fairly smooth. The image variance and mean are an average over the whole image which tends to reduce noise. CTEM phase is not likely to be so well behaved.

A sequence of trial aberration values is shown in Fig. 3 (not the same run as above). Every run will be different, particularly with noise in the image. This graph includes all values in the search and not just the current optimum value. The scatter about the trend line gives some idea of the size of the search volume (i.e. the simplex). The extra activity near trial 300 is the second pass of the simplex method (i.e. the restart), in which the simplex got rebuilt with a large step size. The procedure may converge to a position in which some pairs of aberrations compensate each other, such as a positive $C_{30} = C_{S3}$ being offset by a negative defocus in a local minimum. Fig. 4 shows the final converged aberrations versus the starting errors. The points should lie on the dashed line. Deviation from the dashed line indicates the accuracy of convergence. The two largest deviations are C_{12b} and C_{32b} which are compensation pairs (one positive and one negative).

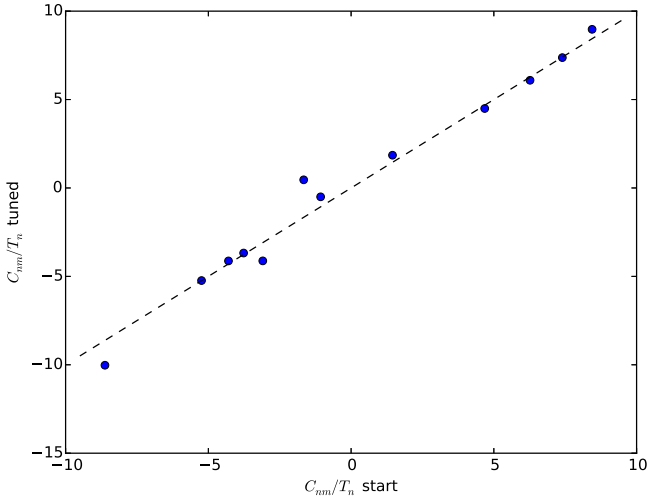

Fig. 4. Final converged aberration values (12 aberrations to third order) versus the known starting error normalized to the tolerance T_n for the run in Fig. 3.

The simplex method is fairly robust but is not known for its fast convergence. To be a worthwhile tuning method this procedure must converge in a reasonable number of iterations (one image per iteration). The approx. number of iterations for a few different orders and starting conditions are shown in Table 2. Order one has three aberrations, order 2 has 7 and order 3 has 12. The number of iterations increases quickly with the number of free parameters (aberrations) and distance from the optimum position. 100 images would be a total of 256x256x100x(16μs) = 105 s. total signal time which is not that extreme. There will also be some time for computer overhead and the number of iterations will vary from specimen to specimen and the starting point. It is technically feasible for the data acquisition system to calculate the sums in Eq. (6) as the image is being acquired and just transmit back to the host computer these two values and not the whole image, which might speed up the process. In practice this method might be applied incrementally to different areas of the specimen if a single location becomes beam damaged (a stable specimen image is required during tuning).

Table 2
Approximate number of test images (may vary with noise and specimen etc.) for the conditions in Fig. 1. Order is n in C_{nm} and range refers to the range of initial errors in the aberration (i.e. a range of 10 means $\pm 10T_n$).

to order n	range	number of images
1	2	50
	5	80
	10	80
2	2	100
	5	150
	10	200
3	2	200
	5	300
	10	400

4. Conclusions

Using a relatively simple normalized image variance offers a possible means of fine tuning or focusing a probe forming aberration corrector in ADF-STEM. Working with the image makes it nearly insensitive to post specimen lens aberrations which might be an advantage. This method probably works best on sturdy thin crystalline specimens (maybe on amorphous thin films) so is complementary to Ronchigram methods that may require changing specimens or moving to an amorphous region of the specimen. Tuning to third order may require many images but has the advantage of working on a crystalline specimen which is frequently the specimen of interest in inorganic materials. Third order tuning is usually not needed often, and second order tuning is faster and adequate in many cases.

This approach has been tested on image simulations. The manufacturers do not provide easy access to sufficient software to easily test this method in practice, but this project should be tried next on a real instrument. Hopefully, this method may find some use in practice in the future.

References

[1] P.W. Hawkes, The correction of electron lens aberrations, Ultramicroscopy 156 (2015) A1–A64.
[2] H.H. Rose, Historical aspects of aberration correction, J. Electron Microsc. 58 (2009) 77–85.
[3] S. Uhlemann, M. Haider, Residual wave aberrations in the first spherical aberration corrected transmission electron microscope, Ultramicroscopy 72 (1998) 109–119.
[4] H. Sawada, T. Sasaki, F. Hosokawa, S. Yuasa, M. Terao, M. Kawazoe, T. Nakamichi, T. Kaneyama, Y. Kondo, K. Kimoto, K. Suenaga, Higher-order aberration corrector for an image-forming system in a transmission electron microscope, Ultramicroscopy 110 (2010) 958–961.
[5] O.L. Krivanek, N. Dellby, A.R. Lupini, Towards sub-Å electron beams, Ultramicroscopy 78 (1999) 1–11.
[6] N. Dellby, O.L. Krivanek, P.D. Nellist, P.E. Batson, A.R. Lupini, Progress in aberration-corrected scanning transmission electron microscopy, J. Electron Microsc. 50 (2001) 177–185.
[7] H. Sawada, T. Sannomiya, F. Hosokawa, T. Nakamichi, T. Kaneyama, T. Tomita, Y. Kondo, T. Tanaka, Y. Oshima, Y. Tanishiro, K. Takayanagi, Measurement method of aberration from Ronchigram by autocorrelation, Ultramicroscopy 108 (2008) 1467–1475.
[8] H. Sawada, M. Watanabe, I. Chiyo, Ad hoc auto-tuning of aberrations using high-resolution STEM images by autocorrelation function, Microsc. Microanal. 18 (2012) 705–710.
[9] A.R. Lupini, S.J. Pennycook, Rapid autotuning for crystalline specimens from an inline hologram, J. Electron Microsc. 57 (2008) 195–201.
[10] A.R. Lupini, P. Wang, P.D. Nellist, A.I. Kirkland, S.J. Pennycook, Aberration measurement using the Ronchigram contrast transfer function, Ultramicroscopy 110 (2010) 891–898.
[11] A.R. Lupini, The electron Ronchigram, in: S.J. Pennycook, P.D. Nellist (Eds.), Scanning Transmission Electron Microscopy, Imaging and Analysis, Springer, New York, 2011, pp. 117–482.
[12] O.L. Krivanek, G.J. Corbin, N. Dellby, B.F. Elson, R.J. Keyse, M.F. Murfitt, C.S. Own, Z.S. Szilagi, J.W. Woodruff, An electron microscope for the aberration-corrected era, Ultramicroscopy 108 (2008) 179–195.
[13] R. Erni, Aberration-Corrected Imaging in Transmission Electron Microscopy, 2nd, Imperial College Press, London, 2015.
[14] E.J. Kirkland, On the optimum probe in aberration corrected ADF-STEM, Ultramicroscopy 111 (2011) 1523–1530.
[15] E.J. Kirkland, Computation in electron microscopy, Acta Cryst. A 72 (2016) 1–27.
[16] S.J. Erasmus, K.C.A. Smith, An automatic focusing and astigmatism correction system for the SEM and CTEM, J. Microsc. 127 (1982) 185–199.
[17] W.O. Saxton, D.J. Smith, S.J. Erasmus, Procedures for focusing, stigmating and alignment in high resolution electron microscopy, J. Microsc. 130 (1983) 187–201.
[18] E.J. Kirkland, An image and spectrum acquisition system for a VG HB501 STEM using a color graphics workstation, Ultramicroscopy 32 (1990) 349–364.
[19] M.J.D. Powell, An efficient method for finding the minimum of a function of several variables without calculating derivatives, Comput. J. 7 (1964) 155–162.
[20] J.A. Nedler, R. Mead, A simplex method for function minimization, Comput. J. 7 (1965) 308–313.
[21] E.J. Kirkland, Advanced computing in electron microscopy, 2nd, Springer, New York, 2010.